

# Numb Regulates the Polarized Delivery of Cyclic Nucleotide-Gated Ion Channels in Rod Photoreceptor Cilia

Vasanth Ramamurthy,<sup>1,2</sup> Christine Jolicoeur,<sup>1</sup>  Demetra Koutroumbas,<sup>1,3</sup> Johanna Mühlhans,<sup>4</sup> Yun-Zheng Le,<sup>5</sup> William W. Hauswirth,<sup>6</sup>  Andreas Giessl,<sup>4</sup> and Michel Cayouette<sup>1,2,3,7</sup>

<sup>1</sup>Institut de recherches cliniques de Montreal, Montreal, Quebec H2W 1R7, Canada, <sup>2</sup>Division of Experimental Medicine and <sup>3</sup>Department of Anatomy and Cell Biology, McGill University, Montreal, Quebec H3A 2B2, Canada, <sup>4</sup>Department of Biology, Animal Physiology, University of Erlangen-Nuremberg, 91058 Erlangen, Germany, <sup>5</sup>Department of Medicine and Harold Hamm Diabetes Center, University of Oklahoma Health Sciences Center, Oklahoma City, Oklahoma 73104, <sup>6</sup>Department of Ophthalmology and Powell Gene Therapy Center, University of Florida, Gainesville, Florida 32610, and <sup>7</sup>Department of Medicine, Université de Montréal, Montreal, Quebec, H3T 1P1 Canada

The development and maintenance of protein compartmentalization is essential for neuronal function. A striking example is observed in light-sensing photoreceptors, in which the apical sensory cilium is subdivided into an inner and outer segment, each containing specific proteins essential for vision. It remains unclear, however, how such polarized protein localization is regulated. We report here that the endocytic adaptor protein Numb localizes to the inner, but not the outer segment of mouse photoreceptor cilia. Rod photoreceptor-specific inactivation of *numb in vivo* leads to progressive photoreceptor degeneration, indicating an essential role for Numb in photoreceptor cell biology. Interestingly, we report that loss of Numb in photoreceptors does not affect the localization of outer segment disk membrane proteins, such as rhodopsin, Peripherin-rds, Rom-1, and Abca4, but significantly disrupts the localization of the rod cyclic nucleotide-gated (Cng) channels, which accumulates on the inner segment plasma membrane in addition to its normal localization to the outer segments. Mechanistically, we show that Numb interacts with both subunits of the Cng channel and promotes the trafficking of Cnga1 to the recycling endosome. These results suggest a model in which Numb prevents targeting of Cng channels to the inner segment, by promoting their trafficking through the recycling endosome, where they can be sorted for specific delivery to the outer segment. This study uncovers a novel mechanism regulating polarized protein delivery in light-sensing cilia, raising the possibility that Numb plays a part in the regulation of protein trafficking in other types of cilia.

**Key words:** cilia; *numb*; photoreceptors; polarity; retina; trafficking

## Introduction

Neuronal function critically depends on the establishment and maintenance of different cellular compartments containing a specific set of proteins. One of the most striking examples of polarized protein localization is observed in photoreceptor cells of the mammalian retina. The light-sensing cilium, which forms the apical domain, is subdivided into two parts: the inner segment (IS), where protein synthesis takes place, and the outer

segment (OS), where proteins of the phototransduction cascade specifically localize (Fig. 1A).

Much has been learned over the past years on the mechanisms regulating the transport of the photopigment rhodopsin to the OS (Sung and Chuang, 2010; Deretic and Wang, 2012), but less is known about how other OS-specific proteins are trafficked. Although it was originally proposed that other OS proteins might “piggyback” on rhodopsin and be transported along the same route (Papermaster, 2002), various evidence suggest that this is most likely not the case. First, many mouse mutants presenting rhodopsin trafficking defects have normal localization of other OS proteins (Insinna and Besharse, 2008; Sung and Chuang, 2010). Second, artificial detachment of the OS leads to accumulation of rhodopsin and the structural OS protein Peripherin/rds in the IS, but at different subcellular locations (Fariss et al., 1997; Lee et al., 2006). Although these observations suggest the existence of alternative sorting mechanisms for other OS proteins, these remain to be identified.

The cyclic nucleotide-gated (Cng) channel specifically localizes to the OS and plays a key part during phototransduction by closing in response to light to prevent  $\text{Ca}^{2+}$  and  $\text{Na}^{+}$  influx and trigger hyperpolarization. Unlike rhodopsin, which localizes to the disk membranes of OS, the Cng channel localizes on the

Received May 13, 2014; revised Aug. 14, 2014; accepted Sept. 9, 2014.

Author contributions: V.R. and M.C. designed research; V.R., C.J., D.K., J.M., and A.G. performed research; Y.Z.-L. and W.W.H. contributed unpublished reagents/analytic tools; V.R., C.J., A.G., and M.C. analyzed data; V.R. and M.C. wrote the paper.

This work was supported by operating grants from the Canadian Institutes of Health Research and the Foundation Fighting Blindness Canada. V.R. received studentships from the Foundation Fighting Blindness Canada and the Fonds de recherche du Québec-Santé. M.C. is a Senior Fellow of the Fonds de recherche du Québec-Santé/Fondation Antoine-Turmel. We thank Robert Molday for the Cnga1, Abca4, Rom-1, Peripherin/rds, and rhodopsin antibodies, Stylianos Michalakis for the Cngb1 antibody, and Jeremy Nathans for the photoreceptor-specific cadherin antibody; Nadja Schröder-Kreβ for technical assistance with EM, Marie-Claude Bélanger for help with *in vivo* electroporations, and Jessica Barthe and Marie-Andrée Marcotte for animal colony management.

The authors declare no competing financial interests.

Correspondence should be addressed to Dr Michel Cayouette, IRCM, 110 Avenue des Pins Ouest, Montreal, QC H2W 1R7, Canada. E-mail: michel.cayouette@ircm.qc.ca.

DOI:10.1523/JNEUROSCI.1938-14.2014

Copyright © 2014 the authors 0270-6474/14/3413976-12\$15.00/0

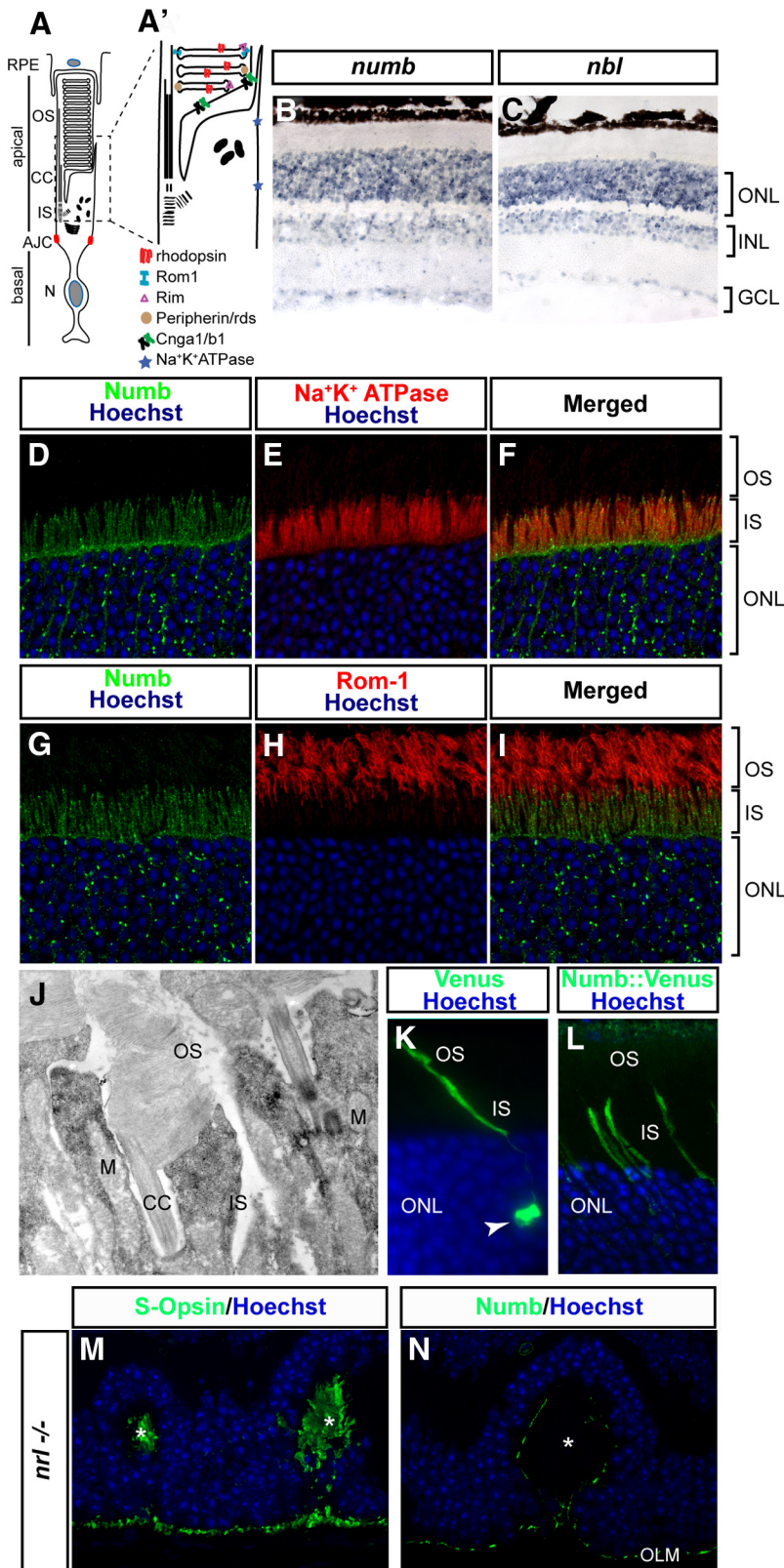


**Figure 1.** Numb/Nbl expression in the adult retina. **A**, Schematic representation of a rod photoreceptor cell depicting the apical and basolateral membrane separated by the apical junctional complex (AJC). **A'**, A magnified view of the region boxed in **A** showing subcellular localization of some proteins studied in this study. RPE, Retinal pigmented epithelium; CC, connecting cilium; N, nucleus; S, synaptic terminal. **B**, **C**, *In situ* hybridization with antisense probes for *numb* and *nbl* on mouse retinal sections at P60. Specific signal is seen in the outer nuclear layer (ONL), inner nuclear layer (INL), and ganglion cell layer (GCL). The ONL contains cell bodies of photoreceptors, whereas the INL contains cell bodies of interneurons and Müller glia. **D–I**, Coimmunostaining of mouse retinal sections at P60, as indicated. **J**, Electron micrographs of immuno-

plasma membrane surrounding the OS (Fig. 1A'). The functional channel is composed of three  $\alpha$  (Cnga1) and one  $\beta$  (Cngb1) subunit in rod photoreceptors (Zhong et al., 2002), and although formation of a heteromeric complex, as well as the adaptor protein Ankyrin-G, were shown to be required for its transport to the OS (Hüttel et al., 2005; Zhang et al., 2009; Kizhatil et al., 2009), the mechanisms controlling the sorting and exclusive polarized localization of the channel to the OS plasma membrane remain unknown.

Recently we reported that the endocytic adaptor protein Numb, which is known to bind the endocytic protein Eps15 and the clathrin adaptor AP-2 (Salcini et al., 1997; Santolini et al., 2000), is essential for the production of terminal asymmetric cell divisions in the developing mouse retina (Kechad et al., 2012). During the course of this study, we noted that Numb expression is maintained in adult photoreceptors, and whereas Numb function has been extensively studied during development, its role in mature neurons *in vivo* remains largely unknown. We report here that Numb and its homolog Numbl like (Nbl) are essential for photoreceptor cell survival and for the polarized sorting of Cng channels to the OS. We find that Numb interacts with both subunits of the rod Cng channel, and promotes trafficking of Cnga1 to the recycling endosome. In the absence of Numb, the Cng channel is no longer exclusively localized to the OS, and additionally accumulates on the IS plasma membrane. Together, these results suggest a model in which Numb functions as an adaptor protein regulating the efficient targeting of the Cng channel to the recycling endosome, where it can be sorted for specific delivery to OS plasma membrane.

← staining for Numb on P60 retinas. DAB precipitates were silver intensified and appear as black dots on the image. Numb is found throughout the IS, but not the OS or CC and mitochondria (M). **K**, **L**, *In vivo* electroporation of a control Venus protein (**K**) or a Numb::Venus fusion (**L**) in photoreceptor cells at P30. Venus is found in the cell body (arrow), as well as the IS and OS, whereas Numb::Venus localizes only in the IS. **M**, S-Opsin staining in *Nrl* knock-out (*nrl*<sup>-/-</sup>) retinas. These retinas contain only cones that often organize in rosettes (asterisks), in which the IS/OS are found. The cone OS are identified by S-Opsin signal in the rosettes (asterisks). **N**, In contrast, no Numb staining is observed in the IS/OS regions of *nrl*<sup>-/-</sup> retina (asterisk). The only Numb staining observed is in the outer limiting membrane (OLM), which is also observed in wild-type retinas.

**Table 1. Primary antibodies used in this study**

Antigen	Antibody name	Species	Dilution	Source	References (if any)
rhodopsin	4D2	Mouse	1/20 (I)	R. Molday (UBC, Vancouver, Canada)	(Hicks and Molday, 1986)
Cnga1	Pmc1d1	Mouse	1/20 (I); 1/30 (W); 10 ml (IP); 1:20–50 (IEM)	R. Molday	(Cook et al., 1989)
Abca4	3F4	Mouse	1/20 (I)	R. Molday	(Illing et al., 1997)
Rom1	1D5	Mouse	1/20 (I)	R. Molday	(Moritz and Molday, 1996)
Peripherin/rds	Per5H2	Mouse	1/20 (I)	R. Molday	(Connell et al., 1991)
Actin		Mouse	1/10,000 (W)	Sigma-Aldrich, A5441	
Na <sup>+</sup> /K <sup>+</sup> ATPase		Mouse	1/100 (I)	Thermo Scientific, MA3-915	
Numb		Rabbit	1/100 (I); 1 μg/ml (W)	Abcam, 14140	
Pr-cadherin		Rabbit	1/100 (I)	J. Nathans (Johns Hopkins University, Baltimore, MD)	(Rattner et al., 2001)
GFP/Venus		Rabbit	1/1000 (I); 1/5000 (W); 3 μg (IP)	Invitrogen, A11122	
Cngb1		Rabbit	1/500 (I)	S. Michalakakis (Ludwig-Maximilians-Universität München, Munich, Germany)	(Hüttel et al., 2005)

Dilutions used for immunostaining (I), Western blotting (W), immunoprecipitation (IP) and immunoelectron microscopy (IEM) are shown.

## Materials and Methods

### Animals

All animal work was carried in accordance with the Canadian Council on Animal Care guidelines. The Opsin-Cre (Le et al., 2006) and *numb/nbl* floxed (Wilson et al., 2007) mouse lines were used to generate photoreceptor-specific cDKO. Both heterozygotes and Cre-negative animals were used as controls in this study and referred to as “control” throughout the text and figures. Animals of either sex were used in this study.

### Probes and in situ hybridization

Digoxigenin-labeled RNA probes were synthesized from full-length cDNA template of *numb* and *numlike*. Eyes were collected, fixed in PFA 4% overnight, frozen in OCT, sectioned, and air-dried for 30 min. Hybridization was done at 65°C overnight with 300 ng/ml of RNA probes in the hybridization buffer (50% formamide, 5× SSC, 5× Denhardt's, 5 mg/ml of Torula RNA, 500 μg/ml fish sperm DNA). The probes were detected with an anti-Dig-AP antibody (1:3500, Roche). The AP activity was revealed using the nitro blue tetrazolium chloride/5-bromo-4-chloro-3'-indolylphosphate substrate (NBT/BCIP, Roche).

### Histology, immunohistochemistry, and electron microscopy

PFA was used as a fixative for all histology and immunohistochemistry, with the exception of tissue used for EM. Eyes were enucleated and fixed by immersion in freshly prepared 4% paraformaldehyde in PBS for 3 h on ice, cryoprotected in sucrose 20% overnight, and cryosectioned. Sections were preincubated for 1 h in blocking buffer (20% goat serum in 0.2% Triton) and then incubated overnight at 4°C with the primary antibodies (Table 1). The Numb antibody used (Abcam) also cross-reacts with Nbl (Kechad et al., 2012).

### Electron microscopy

Retinas from adult mice [postnatal day (P)150] were dissected, cut into small pieces, and fixed in 2.5% glutaraldehyde in 0.1 M sodium cacodylate buffer with 4% sucrose overnight at 4°C. The next day, the tissues were washed with 0.1 M sodium cacodylate buffer, and postfixed in cold 1% buffered OsO<sub>4</sub> and 1.5% aqueous potassium ferrocyanide for 2 h at 4°C. Then, tissues were dehydrated in increasing concentrations of acetone and embedded in Epon 812. Sectioning for electron microscopy examination followed standard procedures on an ultramicrotome (Reichert Ultra Cut AV Ultramicrotome). Blocks of retinas were then cut again and thin sections (60–80 nm thick) were stained in 4% uranyl acetate for 5 min, Reynolds' lead for 3 min, and viewed under a transmission electron microscope (FEI, Titan Krios).

### Pre-embedding immunoelectron microscopy

Vibratome sections were blocked in 10% normal goat serum and 1% bovine serum albumin in PBS for 2 h. Sections were incubated with the primary antibody for 4 d at 4°C. After four 15 min PBS washes, binding of the primary antibody was visualized with a biotinylated goat anti-rabbit IgG (or anti-mouse IgG) secondary antiserum (Vector Laboratories) diluted 1:100 and a peroxidase-based enzymatic detection system (Vec-

tastain Elite ABC kit; Vector Laboratories). The provided avidin-biotin HRP complex (ABC) binds the biotinylated secondary antibodies. This immunocomplex was visualized by adding 0.01% hydrogen peroxide to a 0.05% 3,3'-diaminobenzidine (DAB) solution. The staining was fixed by incubation in 2.5% glutaraldehyde in cacodylate buffer (0.1 M, pH 7.4) for 1 h. DAB precipitates were silver intensified and sections were finally incubated in 0.5% OsO<sub>4</sub> in cacodylate buffer for 30 min at 4°C. After washing and dehydration, vibratome sections were flat-mounted between two sheaths of heat-resistant transparency film in Epon. Ultrathin sections were examined and photographed with a Zeiss EM10 electron microscope and a GATAN SC1000 Orius™ CCD camera in combination with the DigitalMicrograph™ software (GATAN). Images were adjusted for contrast and brightness using Adobe Photoshop CS6.

### In vivo electroporation

DNA preparations were injected subretinally at P0 according to a modified procedure previously described (Matsuda and Cepko, 2004). The volume of the injection was maintained between 0.5 and 1 μl. After the injection, tweezer-type electrodes, (Gene paddles, 3 × 5 mm Paddles Model 542, Harvard Apparatus) soaked in PBS were placed on either side of the head of the pup and five square pulses of 50 ms duration with 950 ms intervals were applied using a pulse generator (ECM 830 Square Wave Electroporation System, Harvard Apparatus). The eyes were collected at P21, fixed, and processed for immunostaining as described above.

### Transfections and constructs

COS-7 cells were transfected with Lipofectamine using the following constructs: Rab11::DsRed (Addgene plasmid 12679, generated by Richard Pagano, Mayo Clinic and Foundation, Rochester, MN 55905; Choudhury et al., 2002), pCAGS-Cnga1, or Numb::Myc. Cells were fixed 24 h after transfection and stained with anti-Cnga1, and imaged using a Zeiss LSM 710 confocal microscope or Leica epifluorescence microscope followed by image deconvolution.

### Quantification

**Photoreceptor cell count.** The number of photoreceptors in the control and cDKO were quantified by averaging the total number of cells in a 200 μm region taken from the central and peripheral retina on three different retinal sections per animal. Statistical comparisons were done using Student's *t* test.

**IS quantification.** Cnga1 localization in the IS in control and cDKO was quantified by averaging the total number of IS displaying Cnga1 labeling on three different retinal sections per animal. IS was identified using morphology. Statistical comparisons were done using Student's *t* test.

**Fluorescence intensity measurements.** Intensity measurements were obtained using the Volocity software (PerkinElmer). Auto-threshold adjustment was applied to the image before the measurement. The experiment was repeated twice and 20–40 cells were analyzed for each condition in every experiment.

### Viral vectors and intraocular injections

The titer of the AAV vectors used was  $6.36 \times 10^{13}$  pfu/ml and the serotype was AAV5. The procedures for construction and purification of

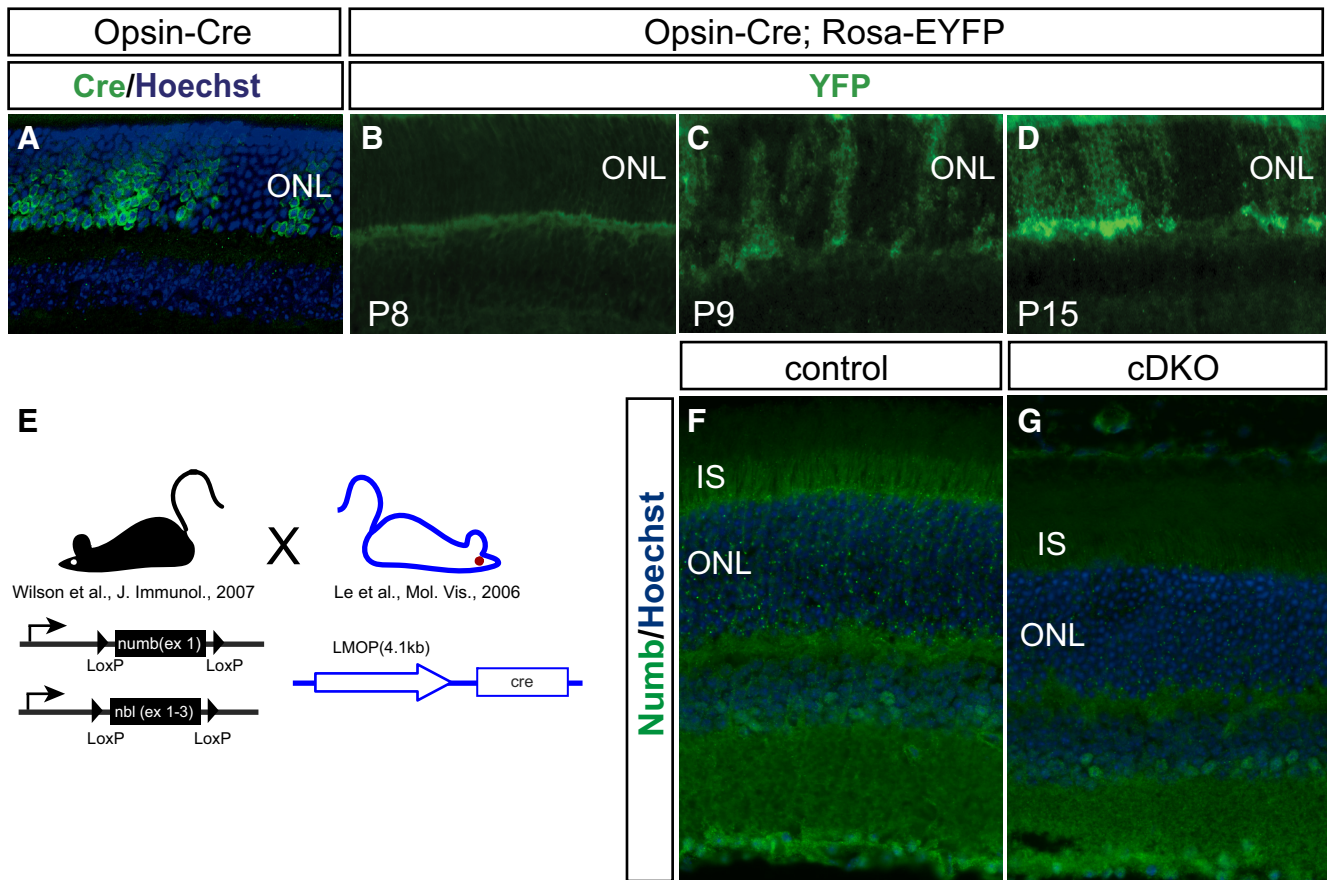


**Figure 2.** Conditional inactivation of Numb/Nbl in photoreceptors. **A**, Immunostaining for Cre on retinal sections of Opsin-Cre mouse at P60. Cre (green) is expressed only in photoreceptor cells located in the ONL. Note the mosaic expression pattern of Cre in the photoreceptor layer. **B–D**, Recombination efficiency in the Opsin-Cre mouse. Immunostaining for YFP on mouse retinal sections of a F1 double-transgenic Opsin-Cre; R26R-EYFP at different stages, as indicated. Recombination, as indicated by YFP expression (green), is mosaic and starts at P9, but is more robust by P15. **E**, A diagram illustrating the breeding scheme to generate Numb/Nbl cDKO. **F, G**, Immunostaining for Numb on retinal sections from cDKO at P60. Numb (green) expression is decreased in the cDKO in the apical IS, indicating efficient gene inactivation. For illustration purposes, an area with complete loss of Numb signal was selected, but other areas of the same retina had some Numb staining remaining, as expected due to mosaicism of Cre activity shown in **A–D**. Sections were counterstained with Hoechst (blue) to reveal nuclei in **A, F**, and **G**.

adenoviral vectors and intraocular injections was described previously (Flannery et al., 1997). The volume of the injection was maintained between 0.5 and 1  $\mu$ l. Animals were injected with AAV-Cre-GFP into one eye and received a control injection of vehicle or AAV-GFP into the contralateral eye.

*Protein extraction, immunoblotting, and immunoprecipitation*

Cells were harvested, and lysed in a NP-40 buffer: 50 mM TRIS, pH 8.0, 150 mM NaCl, 1.0% NP-40 with Complete Protease Inhibitor Cocktail (Roche). For immunoblotting, 100  $\mu$ g of protein samples were separated by electrophoresis on a 10% SDS-PAGE gels and then transferred onto PVDF membranes (Millipore). The membranes were blocked with 5% milk in TBST (pH 8.0, 0.1% Triton). Immunoblotting with the primary antibody (Table 1) was performed at 4°C overnight in 0.5% dry milk in TBST. The primary antibody was detected with an HRP-conjugated goat anti-rabbit (1: 10,000; Jackson Immunoresearch) in 0.5% dry milk in TBST. Detection of bound antibodies was visualized with the ECL kit (GE Life Science).

For immunoprecipitation (IP), Dynabeads Magnetic Beads (Dynabeads Protein G, Invitrogen) were used according to manufacturer’s specification. Briefly, 40  $\mu$ l of beads were incubated with primary antibody (Table 1) for 1 h at 4°C. 1 mg of cell lysate was incubated with the bead-antibody mixture in Iph Buffer (50 mM Tris pH 8.0, 150 mM NaCl, 5 mM EDTA, 0.1% NP-40) overnight at 4°C. The beads were separated using a magnet (MagnaBind, Pierce) and washed in Iph Buffer. The beads were then boiled in 2 $\times$  Laemmli buffer at 95°C for 10 min and the supernatant was used for immunoblotting as described above.

**Results**

**Numb and Nbl are expressed in photoreceptors**

We found that both *numb* and *nbl* mRNA are expressed in all cell layers of the adult retina, but particularly enriched in the photoreceptor layer (Fig. 1B,C). In photoreceptors, the Numb protein was strikingly polarized in a subdomain of the sensory cilium, which matched the IS marker Na<sup>+</sup>/K<sup>+</sup> ATPase, but did not overlap with the OS marker Rom-1 (Fig. 1D–I). Consistently, immuno-EM revealed no signal for Numb in the OS, but strong localization in the IS (Fig. 1J). *In vivo* electroporation of a fluorescently tagged version of Numb (Numb::Venus), which was previously reported to localize like endogenous Numb (Kechad et al., 2012), was also concentrated in the IS and excluded from the cell body and OS, unlike the control Venus protein (Fig. 1K–L), further supporting the immunostaining data. To determine whether Numb is expressed in cone photoreceptors, we stained *nrl* KO retinas, which contain only cones (Mears et al., 2001), thereby facilitating the interpretation of the staining. Interestingly, we did not detect any Numb labeling in cone IS/OS area (Fig. 1M,N), suggesting that Numb is not expressed in cones. Together, these results indicate that both Numb and Nbl are expressed in rod photoreceptors and that Numb is highly polarized in the IS, where protein synthesis takes place.

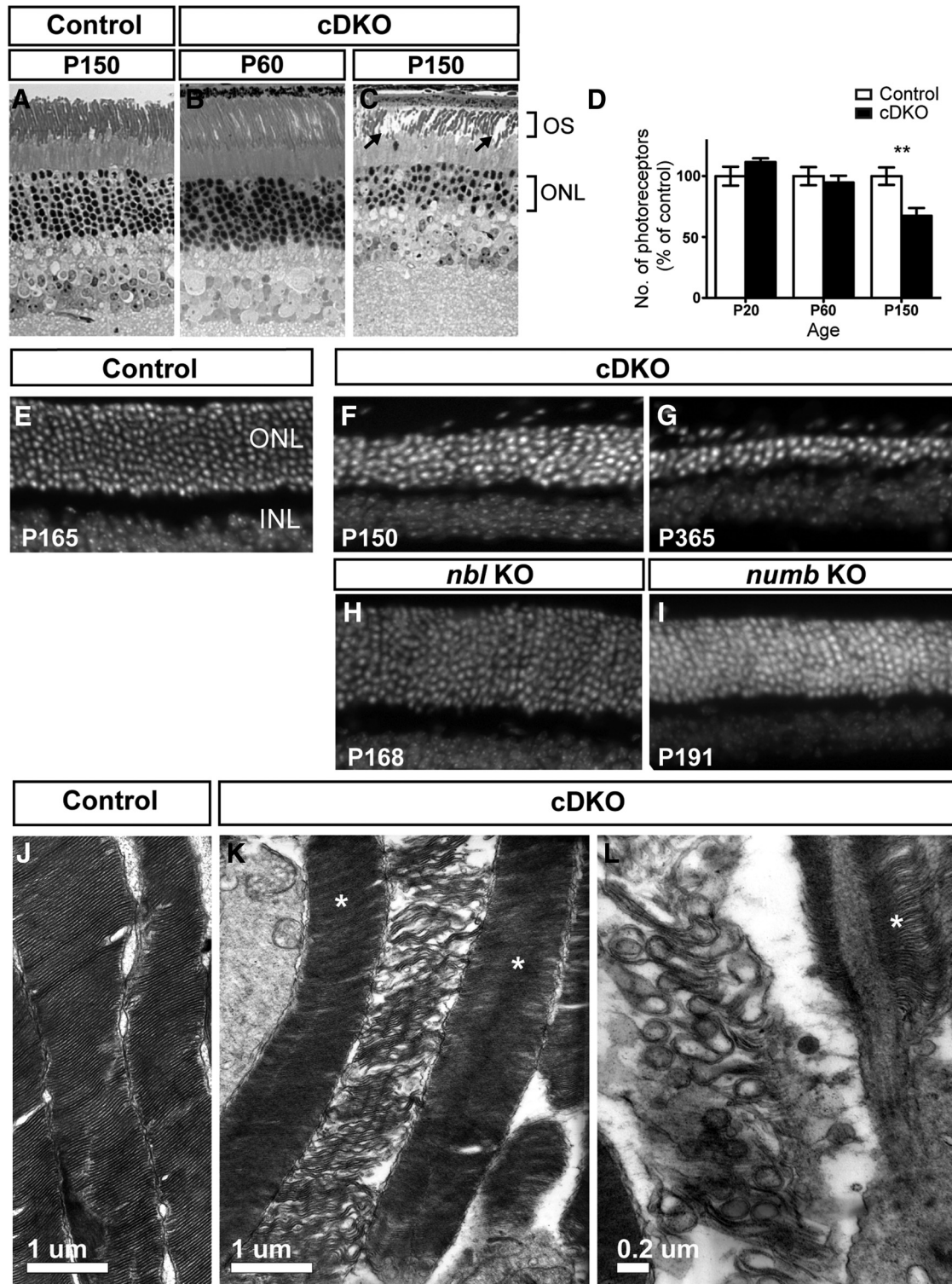


**Figure 3.** Numb/Nbl function is required for rod photoreceptor cell survival. **A–C**, Toluidine blue staining of retinal sections from a Cre-negative (control) mouse at P150 (**A**) and cDKO at P60 (**B**) and P150 (**C**). The cDKO retina appears normal at P60, whereas photoreceptors are degenerating at P150, as shown by the thinning of the ONL, loss of columnar organization of nuclei and degeneration of the OS (**C**, arrows). **D**, Quantification (mean  $\pm$  SEM) of the number of photoreceptors in the cDKO and control retinas at P20, P60, and P150 ( $n = 5$  animals for each time;  $**p = 0.0093$ ; Student's  $t$  test). **E–G**, Retinal sections from control (**E**), cDKO (**F**, **G**), single *nbl* KO (**H**), or *numb* KO (**I**) KO, stained with Hoechst to visualize nuclei at different postnatal days, as indicated. In the cDKO, photoreceptor degeneration is clearly detected by P150 (**F**), but progressively worsens with age and is almost complete by 1 year (**G**), when only two to three rows of photoreceptors are left in the ONL. Single KO mice do not show any signs of photoreceptor degeneration. **J–L**, Electron micrographs of control and cDKO photoreceptor OS. Control OSs (**J**) show regular stacking of disks enclosed within a plasma membrane, but cDKO OSs appear disorganized (**K**, **L**). Note that not all OSs are degenerating at this age (asterisks), most likely reflecting the mosaicism of *numb/nbl* deletion.

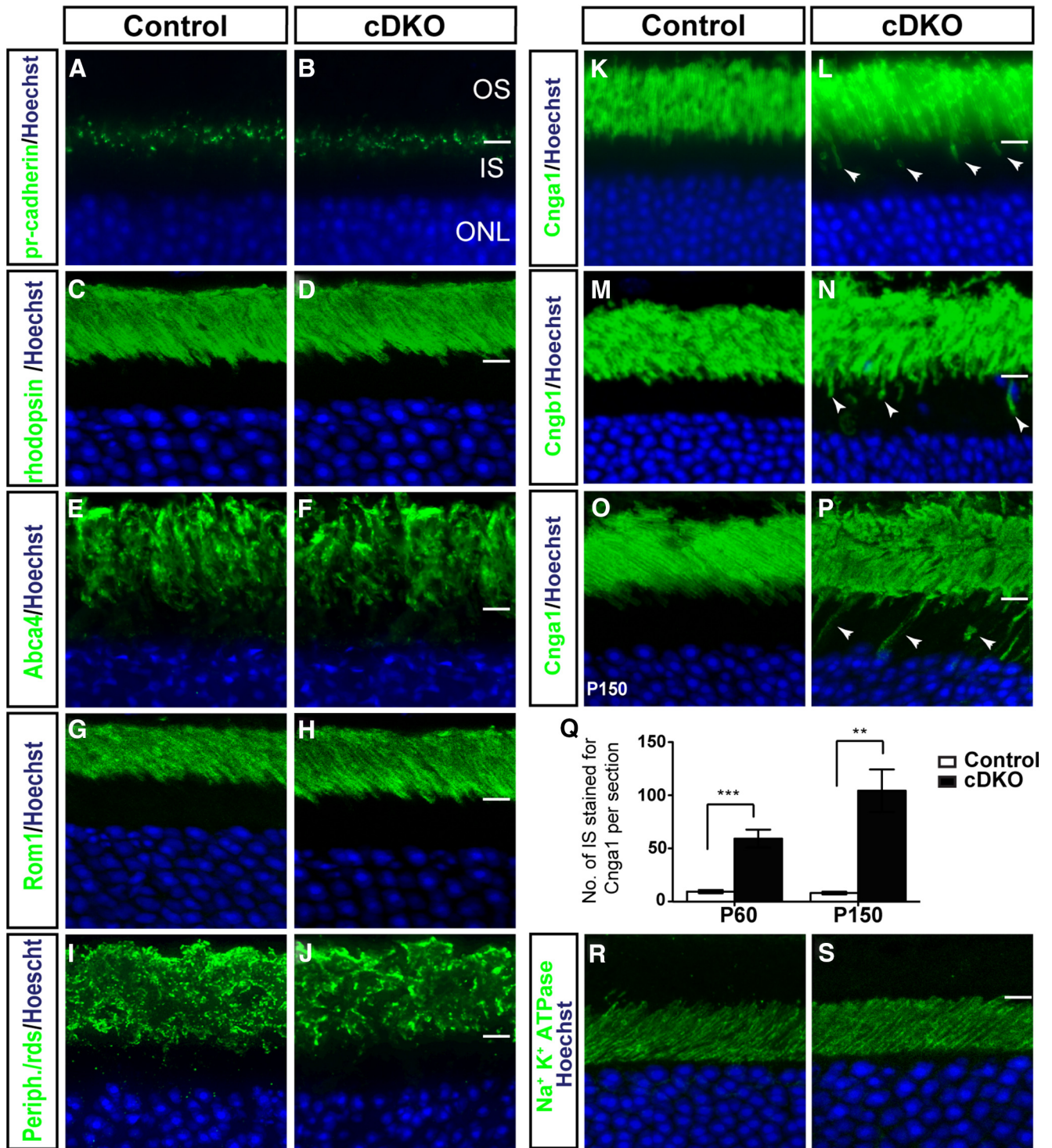


**Figure 4.** Numb/Nbl function is required for the exclusive localization of Cng channels in rod photoreceptor outer segments. *A–P*, Immunostaining of retinal sections from control and cDKO mouse at P60 (*A–N*) and P150 (*O, P*) for photoreceptor-specific cadherin (*A, B*), or various OS markers, as indicated. Although all OS disk membrane proteins studied (rhodopsin, Abca4, Rom1, and Peripherin-rds) localize normally in cDKO, Cnga1 and Cngb1 are abnormally detected in the IS (arrowheads in *L, M, P*), in addition to their normal localization in the OS. *Q*, Quantification of the number of IS with Cnga1 labeling in the IS per retinal section in cDKO compared with wild-type controls at P60 and P150 (mean ± SEM;  $n = 5$  animals; \*\*\* $p = 0.0007$ , \*\* $p = 0.0014$ , Student's *t* test). *R, S*, Immunostaining of P60 retinal sections from control (*R*) and cDKO (*S*) mouse for Na<sup>+</sup>/K<sup>+</sup> ATPase. All sections were counterstained with Hoechst (blue) to reveal nuclei.

**Numb/Nbl function is required for rod photoreceptor cell survival**

As Numb/Nbl function is essential for embryonic development (Zhong et al., 2000; Zilian et al., 2001; Petersen et al., 2002) and normal cell fate decisions in the developing retina (Kechad et al., 2012), we generated a rod photoreceptor-specific knock-out

mouse using the Opsin-Cre mouse line (Le et al., 2006). As expected, this line produced specific, albeit mosaic, recombination in rod photoreceptors from as early as P9 (Fig. 2*A–D*). We then crossed the Opsin-Cre mouse with a line carrying floxed alleles for both *numb* and *nbl* (Wilson et al., 2007) to generate conditional double knock-outs (cDKO). As expected, Numb immuno-

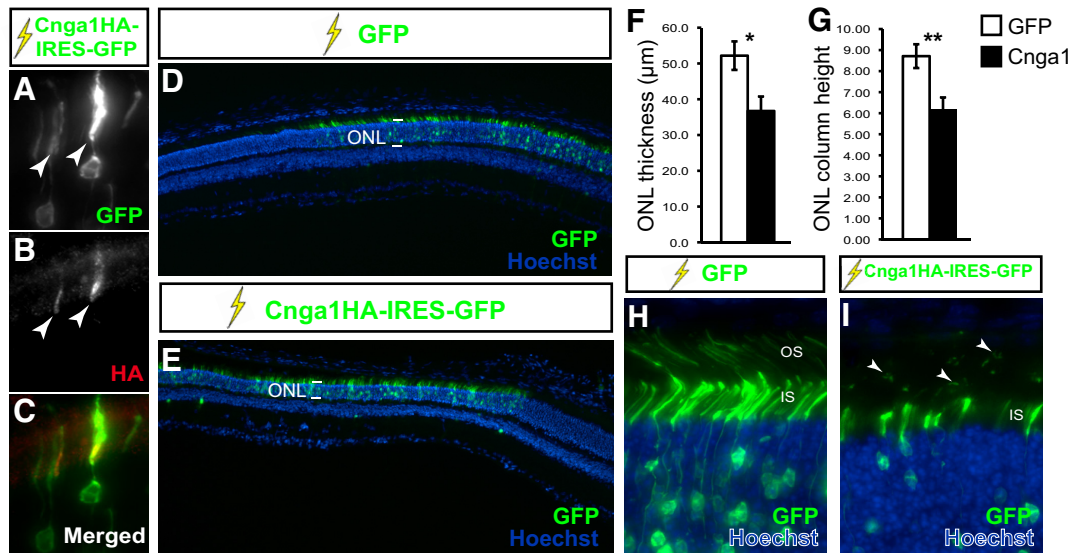


**Figure 5.** Overexpression of Cnga1 in wild-type photoreceptors induces degeneration. *A–C*, *In vivo* electroporation (lightning sign) of photoreceptors with a construct expressing both an HA-tagged version of mouse Cnga1 (Cnga1HA) and GFP from an internal ribosome entry site (IRES), stained for HA. Transfected photoreceptors expressing GFP (*A*) show accumulation of Cnga1HA in the IS, as seen by HA staining (*B*). *D, E*, A low-magnification image of a region of the retina transfected with GFP (*D*) or with Cnga1HA-IRES-GFP (*E*) constructs 3 weeks after electroporation. The GFP staining identifies transfected cells. The thickness of the ONL, which contains photoreceptors, is much reduced in the Cnga1-transfected regions (compared bracketed area in *D* and *E*). *F, G*, Quantification of the ONL thickness in GFP- or Cnga1-transfected areas expressed both in  $\mu\text{m}$  (*F*; ONL thickness) and as number of rows of photoreceptor nuclei (*G*; ONL column height). Both methods show significant reduction of ONL thickness after overexpression of Cnga1 (mean  $\pm$  SEM; \* $p = 0.04$ , \*\* $p = 0.01$ , Student's *t* test;  $n = 4$  GFP and 5 Cnga1-transfected retinas). High magnification view of photoreceptors 3 weeks after electroporation with GFP (*H*) or Cnga1HA-IRES-GFP (*I*) constructs *in vivo*. Cnga1-expressing photoreceptors show fragmented OS (arrowheads), a sign of degeneration.

staining in cDKO photoreceptors was drastically reduced (Fig. 2*E–G*), thereby confirming both the successful generation of a cDKO and the specificity of the antibody.

In cDKO, retinal histology appeared normal within the first 2 months, but disorganized OS and a thinner photoreceptor layer was clearly detected by 5 months of age (Fig. 3*A–D*). The photoreceptor degeneration was progressive and almost complete by 12 months (Fig. 3*E–G*). In contrast, single knock-outs for either *numb* or *nbl* had no signs of photoreceptor degeneration, even in animals older than 5 months (Fig. 3*H, I*), suggesting functional redundancy, as previously reported in other nervous tissues (Petersen et al., 2002, 2004). Closer examination of the cDKO OS by electron microscopy showed various defects ranging from loose stacking of membranes to completely disrupted OS structures (Fig. 3*J–L*). Thus, Numb/NbL function is essential for rod photoreceptor cell survival.

### Numb/NbL function regulates polarized localization of rod cng channels to the OS

How could Numb/NbL inactivation lead to progressive photoreceptor degeneration? Given that Numb/NbL control the maintenance of cadherin-based adhesions in neural progenitors (Rasin et al., 2007), we first asked whether photoreceptor-specific cadherin (pr-cadherin), which is essential for photoreceptor survival (Rattner et al., 2001), might be disrupted in cDKO. Immunostaining on control and cDKO retinal sections, however, did not reveal any obvious changes in the localization or expression level of pr-cadherin (Fig. 4*A, B*), arguing against this possibility.

As abnormal trafficking of OS proteins is known to eventually lead to photoreceptor cell death (Insinna and Besharse, 2008; Ramamurthy and Cayouette, 2009), we next wondered whether protein localization might be affected in cDKO photoreceptors. Because OS degeneration can indirectly lead to accumulation of OS proteins in the IS and cell body, we studied P60 retinas, a stage when degeneration is not yet detected in cDKO (Fig. 3*B, D*).

Whereas proteins normally found on the OS disk membrane, such as rhodopsin, Abca4, Rom-1, and Peripherin/rds localized normally (Fig. 4*C–J*), the OS plasma membrane proteins Cnga1 and Cngb1 abnormally accumulated in the IS of cDKO photoreceptors, in addition to their normal localization in the OS (Fig. 4*K–N*). This accumulation worsened with age and was more drastic by P150 (Fig. 4*O–Q*). We next wanted to determine whether other OS plasma membrane proteins, such as the  $\text{Na}^+/\text{Ca}^{2+}/\text{K}^+$  exchanger, were also mislocalized in cDKO photoreceptors, but this was unfortunately not possible due to the lack of reliable antibodies. Nonetheless, to determine whether any photoreceptor plasma membrane protein trafficking was disrupted, we studied the localization of the  $\text{Na}^+/\text{K}^+$  ATPase, which localizes specifically on the IS plasma membrane, but found no change in cDKO photoreceptors (Fig. 4*R, S*). Together, these results indicate that Numb/NbL function is required to prevent targeting of Cng channels to the IS plasma membrane. Since Cnga1 and Cngb1 are still normally localized in the OS of cDKO, even in photoreceptors showing accumulation in the IS, these results argue against an essential role for Numb in the transport of Cng channels to the OS, and instead point to a role in sorting for the exclusive delivery to the OS plasma membrane.

Because accumulation of Cng channels in the IS is observed before we detect any photoreceptor degeneration in cDKO, we reasoned that mislocalization of Cng channels might actually induce photoreceptor cell death. To test this possibility, we overexpressed Cnga1 in wild-type photoreceptors to produce artificial accumulation in the IS, therefore mimicking the cDKO phenotype. To do this, we electroporated retinas *in vivo* with a construct encoding an HA-tagged version of Cnga1, as well as GFP, from an internal ribosome entry site (Cnga1HA-IRES-GFP), and then studied the effect of Cnga1 overexpression on photoreceptor survival 3 weeks later. As expected, overexpression of Cnga1 led to accumulation in the IS, as seen in GFP-positive transfected cells

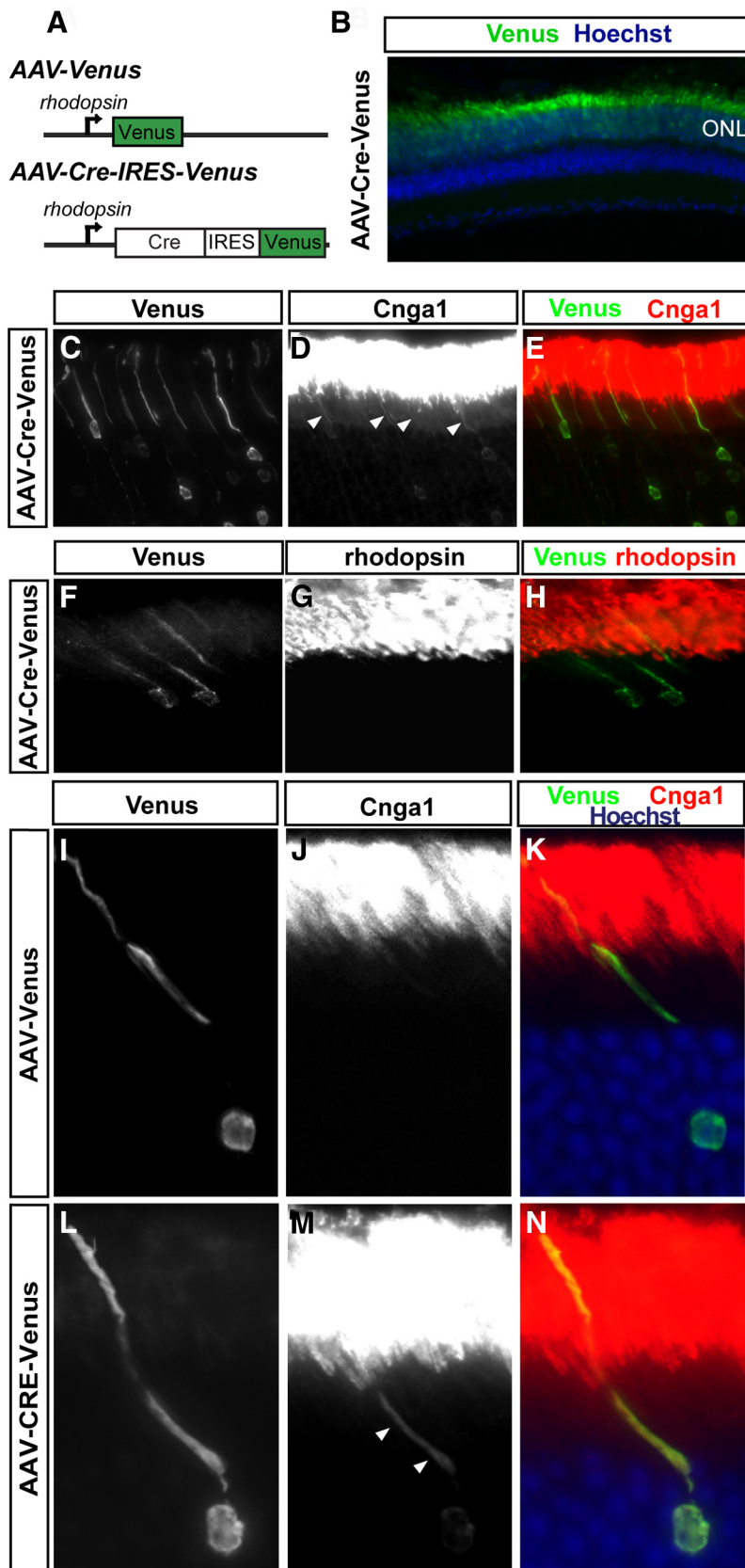


**Figure 6.** Numb/NbL function is required cell autonomously for Cnga1 trafficking. **A**, Schematic representation of the AAV vectors. The 4.1 kb mouse rhodopsin promoter was used to drive Venus alone, or Cre recombinase and Venus using an internal ribosome entry site (IRES). **B–N**, Sections of Numb/Nbl<sup>flox/flox</sup> mouse retina infected with AAV-Venus or AAV-Cre-Venus and immunostained for Venus, Cnga1, and rhodopsin, as indicated. The AAV vectors were injected subretinally at P23 and the retina analyzed 3 weeks later. The AAV vectors specifically infected photoreceptor cells, as seen by specific Venus expression in the ONL (**B**,

stained for HA (Fig. 5A–C). Strikingly, Cnga1-transfected areas showed a significant reduction in photoreceptor cell layer thickness compared with GFP-transfected controls (Fig. 5D–G). Interestingly, Cnga1-overexpressing photoreceptors that were still present 3 weeks after electroporation had abnormal morphology with reduced OS length and fragments of degenerating OS membranes accumulating in the subretinal space (Fig. 5H, I), similar to what we observe in the cDKO retina *in vivo* (see Fig. 3C, I, J). Together, these results suggest that accumulation of Cnga1 in the inner segment is detrimental to photoreceptor survival and eventually leads to cell death.

**Numb/NbL function cell-autonomously to regulate rod cng channel localization to the OS**

Although the above results implicate Numb/NbL function in Cng channel localization, it remained possible that (1) Cng channel mislocalization occurs only in photoreceptors with degenerating OS that could have gone unnoticed in a section containing many thousands of photoreceptors, (2) Numb inactivation from P9 using the Opsin-Cre driver affect OS development in some ways that later lead to abnormal trafficking of the channels, and (3) loss of Numb in a large proportion of photoreceptors cause changes in cell–cell interactions that indirectly affect Cng channel trafficking. To address these issues, we generated adeno-associated viral (AAV) vectors expressing either Venus alone (AAV-Venus) or Cre and Venus (AAV-Cre-IRES-Venus) under the regulation of the rod-specific opsin promoter (Fig. 6A). These vectors allowed us to visualize individual infected cell morphology using the Venus reporter and to control the timing of gene inactivation by introducing the virus into floxed mice at any given stage. To avoid effects of Numb/NbL inactivation on the development of OS, the AAV vectors were injected into the subretinal space of *numb/nbl* floxed mice at P21, a stage when the OS are fully developed, and the retinas were collected

←  
green). AAV-Cre-Venus-infected photoreceptors display a normal morphology, as visualized by Venus expression. Cnga1 (red) labels the outer segments, but also some IS in AAV-Cre-Venus-infected photoreceptors (arrowheads in **D** and **M**), as observed in the cDKO *in vivo*. Noninfected or control-infected photoreceptors do not show accumulation of Cnga1 in the IS (**D**, **J**). AAV-Cre-Venus-infected photoreceptors do not show any mislocalization of rhodopsin (**F–H**). Sections were counterstained with Hoechst (blue) to reveal nuclei in **B**, **K**, and **N**.



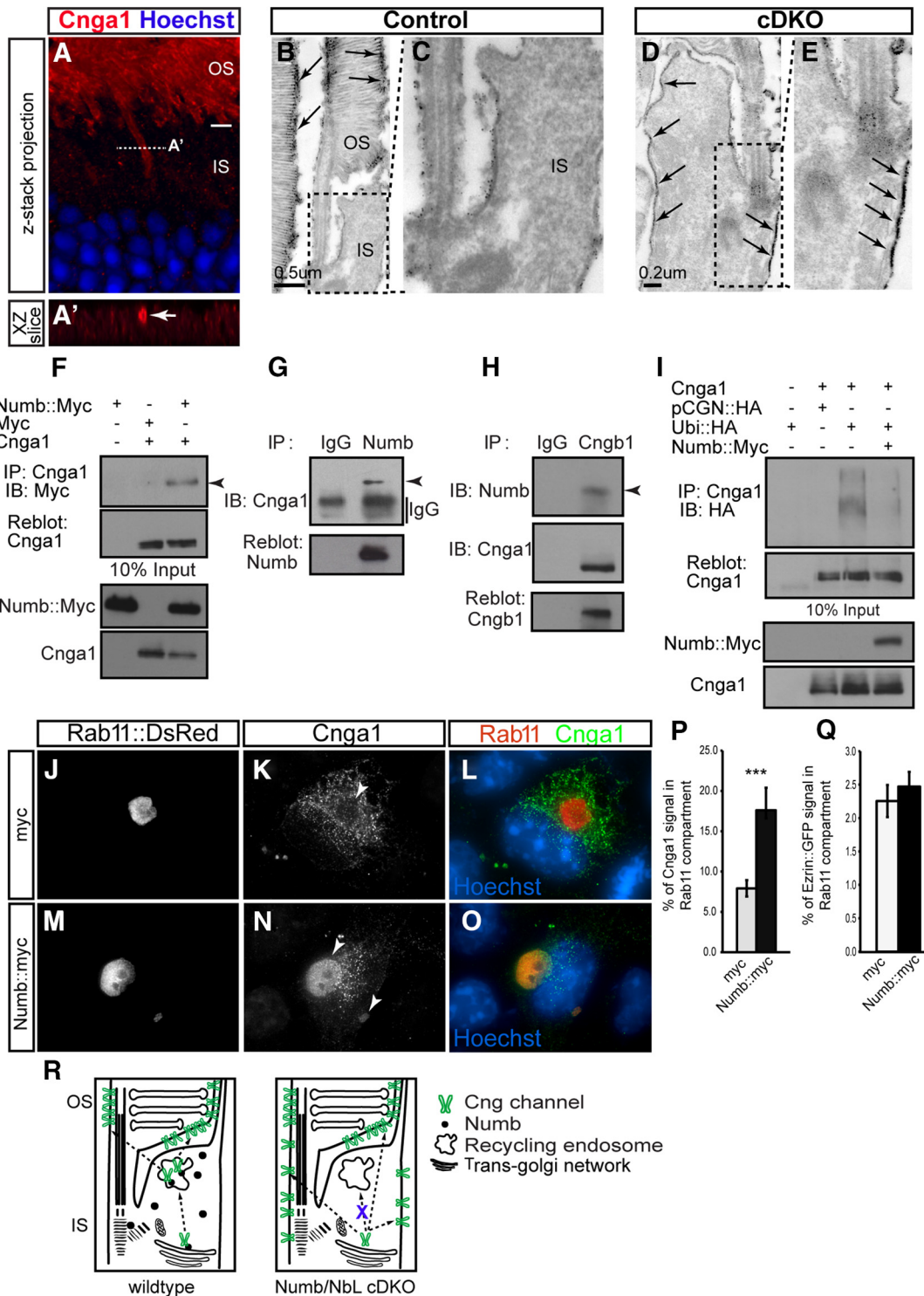


**Figure 7.** Numb interacts with Cng channel subunits and promotes trafficking of Cnga1 to the recycling endosome. **A**, Confocal z-stack projection of a cDKO retinal section at P60 immunostained for Cnga1 (red) and Hoechst (blue). The dotted line indicates the XZ slice view shown in **A'**. Cnga1 accumulates on the outer edge of the IS (arrow). **B–E**, Electron micrographs of control (**B, C**) and cDKO (**D, E**) photoreceptors immunostained for Cnga1 at P60. DAB precipitates were silver intensified and appear as black dots on the image. The boxed areas in **B** and **D** indicate the magnified views shown in **C** and **E**. Cnga1 labeling is indicated by arrows. **F**, Coimmunoprecipitation of Cnga1 and Numb in HEK293 cells. **G**, Coimmunoprecipitation of Cnga1 and Numb *in vivo* at P60. **H**, Coimmunoprecipitation of Numb and Cngb1 *in vivo* at P60. **I**, Pull down of Cnga1 with Ubiquitin-HA (Ubi::HA) in HEK293 cells, in presence of exogenous Numb (Numb::Myc) or not. IB, Immunoblotting. **J–O**, Cos-7 cells cotransfected with Rab11::DsRed and mouse Cnga1, in the presence of exogenous Numb (Numb::myc) or a control empty construct (myc). Cnga1 was detected by immunostaining. The amount of Cnga1 in the recycling endosome (arrowheads) is increased upon Numb overexpression. **P**, Fluorescence intensity measurements of the percentage (%) of Cnga1 signal localized in the Rab11 compartment over the total Cnga1 signal in control transfected (myc) and Numb overexpressing (Numb::myc) Cos-7 cells (mean ± SEM; myc: n = 30 cells; Numb::myc: n = 28 cells; \*\*\*p = 0.002, Student's t test). **Q**, Fluorescence intensity measurements of the percentage (%) of Ezrin::GFP signal localized in the Rab11 compartment in control transfected (myc) and Numb overexpressing (Numb::myc) Cos-7 cells (mean ± SEM; myc: n = 17 cells; Numb::myc: n = 20 cells; \*\*\*p = 0.52, Student's t test). **R**, A model of Numb/Nbl function in photoreceptor cilia. In wild-type photoreceptors (left), Numb interacts with the Cng channels post-Golgi and promotes their trafficking to the recycling endosome, where they are sorted for specific delivery to the OS plasma membrane. In the absence of Numb (right), the Cng channel is not trafficked to the recycling endosome and cannot be sorted, such that it ends up localizing to both the IS and OS plasma membrane.

and analyzed 2–3 weeks later. As expected, the rhodopsin promoter achieved highly specific photoreceptor expression (Fig. 6B). Interestingly, infection of *numb/nbl* floxed photoreceptors with AAV-Cre-IRES-Venus mimicked the phenotype observed in the cDKO mouse retina *in vivo* and led to clear accumulation of Cnga1 in the IS (Fig. 6C–E), whereas rhodopsin localization was not altered (Fig. 6F–H). Remarkably, AAV-Cre appeared much more efficient than the Opsin-Cre cDKO line to inactivate Numb/NbL, as the large majority of infected photoreceptors (GFP-positive) showed accumulation of Cnga1 in the IS ( $74.3 \pm 2.0\%$ ,  $n = 112$  cells from 4 different animals), compared with only 50–100 photoreceptors per retina section showing Cnga1 in the IS in the cDKO (Fig. 4Q). Importantly, the OS was clearly visualized in cells showing accumulation of Cnga1 in the IS and their morphology, as visualized by Venus expression, was indistinguishable from that of controls (Fig. 6C–E). Additionally, infection of wild-type photoreceptors with the same AAV-Cre-IRES-Venus vector did not have any effect on photoreceptor morphology or Cnga1 trafficking (data not shown), excluding the possibility that the injection procedure or expression of Cre indirectly leads to mislocalization of Cnga1. Accumulation of Cnga1 in the IS was also readily observed in isolated Cre-expressing photoreceptors, whereas Venus expression alone did not affect Cnga1 localization (Fig. 6I–N). Together, these results exclude OS developmental defects, degeneration, or noncell autonomous effects as possible explanations for the cDKO phenotypes, indicating that Numb/NbL function cell-autonomously to regulate Cng channel localization.

### Cng channel accumulates on the IS plasma membrane of cDKO rod photoreceptors

We next reasoned that identifying the exact location of Cng channel accumulation in cDKO IS would provide information about a potential mechanism for Numb/NbL function. Detailed analysis of Cnga1 staining using three-dimensional confocal imaging showed concentrations around the edge of the IS, suggesting accumulation on the plasma membrane (Fig. 7A,A'). To confirm this interpretation, we used immunofluorescence. Strong Cnga1 staining was observed along the OS plasma membrane in both wild-type and cDKO photoreceptors (Fig. 7B and data not shown), but Cnga1 signal was additionally found on the IS plasma membrane of cDKO photoreceptors (Fig. 7C–E). These results suggest that Numb/NbL function is not required for the general delivery of Cnga1 to the plasma membrane, but instead that it is essential to restrict delivery to the OS plasma membrane and/or prevent accumulation on the IS membrane.

### Numb physically interacts with cng channel subunits and regulates Cnga1 trafficking to the recycling endosome

Given that Numb is a well known endocytic adaptor protein that interacts with various cargo proteins to regulate their trafficking (Santolini et al., 2000; McGill and McGlade, 2003; McGill et al., 2009), we asked whether it could form a complex with Cng channels. Consistently, we found that Numb and Cnga1 coimmunoprecipitate when exogenously expressed in cell lines (Fig. 7F). To study these interactions *in vivo*, we performed coimmunoprecipitations from protein extracts of adult mouse retina. We found that Cnga1 was pulled-down with an antibody to Numb (Fig. 7G), and conversely, an antibody to Cngb1 was able to pull-down Numb (Fig. 7H), as well as Cnga1, as previously reported (Hüttel et al., 2005). These results suggest that Numb forms a complex with Cnga1 and Cngb1 *in vivo*.

Because Numb was previously reported to interact with ubiquitin ligases (Juven-Gershon et al., 1998; Susini et al., 2001; Nie et al.,

2002) to regulate the degradation of various cargos (Qiu et al., 2000; McGill and McGlade, 2003; Di Marcotullio et al., 2006, 2011; McGill et al., 2009), we first hypothesized that it might promote the local removal of Cng channels from the IS plasma membrane by promoting their ubiquitination and degradation. To test this possibility, we cotransfected HEK293 cells with a HA-tagged ubiquitin (Ubi::HA) together with Cnga1 in the presence or absence of exogenous Numb, immunoprecipitated with Cnga1, and probed the blots for HA. In contrast to what we predicted, however, we found that Numb expression actually decreased the levels of Ubi::HA that coimmunoprecipitated (Fig. 7I), suggesting that Numb reduces Cnga1 degradation, possibly promoting trafficking to another intracellular pathway.

Because the recycling endosome is known for its role as an intermediate sorting station for apical transport (Rodriguez-Boulan and Macara, 2014), we hypothesized that the presence of Numb might promote trafficking of Cng channels to the recycling endosome. To study the role of Numb on the trafficking of Cng channel, we cotransfected Cnga1 or the cytoplasmic peripheral membrane protein Ezrin::GFP as control, together with a fluorescent fusion construct for the recycling endosome (Rab11::DsRed), and either control empty vector (myc) or exogenous Numb (Numb::myc) in COS-7 cells. Interestingly, we found that although only a small fraction of Cnga1 localized to Rab11-positive compartments in myc-transfected or nontransfected cells, we observed a significant increase in the amount of Cnga1 in the Rab11 compartments in Numb-overexpressing cells (Fig. 7J–P). In contrast, Numb overexpression did not affect the trafficking of Ezrin::GFP (Fig. 7Q). Interestingly, accumulation of Cnga1 in Rab11-positive endosomes was often accompanied by a general decrease of Cnga1 levels in the rest of the cell (Fig. 7M–O), suggesting a redirection of Cnga1 from other compartments to the recycling endosome in the presence of Numb. These results indicate that Numb regulates the trafficking of Cnga1 to the recycling endosome and, together with our *in vivo* findings, suggest that this is an important step in preventing Cng channels from being targeted to the IS plasma membrane, and for the specific and exclusive delivery to the OS plasma membrane.

## Discussion

Abnormal trafficking of ciliary proteins is a major cause of a class of human diseases known as ciliopathies, but the molecular mechanisms regulating polarized protein transport to cilia remain largely unknown. In this study, we used mouse genetics to uncover a novel function for Numb in the polarized delivery of ion channels to photoreceptor cilia. These results could have important consequences in our understanding of some retinal degenerative diseases and other ciliopathies. We discuss these implications below.

A particularly important finding in this study is the progressive photoreceptor degeneration observed in cDKO retinas, which identifies Numb as a key regulator of photoreceptor cell homeostasis and survival. While the exact cause of photoreceptor cell death remains unclear, accumulation of Cng channels on the IS plasma membrane might cause overactivation of the channel, which could raise intracellular  $Ca^{2+}$  concentrations and lead to cell death (Fox et al., 1999; Vallazza-Deschamps et al., 2005). Future investigations using  $Ca^{2+}$  imaging in cDKO photoreceptors might help address this question directly. Nonetheless, our finding that overexpression of Cnga1 in wild-type photoreceptors induces degeneration is consistent with the possibility that accumulation of Cnga1 on the IS plasma membrane in Numb/NbL cDKO is detrimental to photoreceptor survival. Photoreceptor degeneration in the cDKO retina might also be indirect. Indeed, a number of reports have linked intracellular accumulation of rhodopsin and the consequent production of oxidative

damage with retinal degenerations (Nir and Papermaster, 1989; Agarwal et al., 1990; Nir et al., 1990; Chinchore et al., 2009). Because rhodopsin (and many other disk membrane proteins) eventually accumulates in the IS of old Numb/NbL cDKO retinas (>P150; data not shown), most likely as a consequence of the degenerated OS, rhodopsin-mediated toxicity could be involved in the photoreceptor cell death of Numb/NbL cDKO.

Progressive photoreceptor cell loss, as observed in Numb/NbL cDKO, is a hallmark of several retinal degenerative diseases in humans (Li, 2001; Hartong et al., 2006). This raises the interesting possibility that mutations in *numb* and/or *nbl* might contribute to human diseases. Human *NUMB* maps to chromosome 14q24.3 and, interestingly, a 10-cM region overlapping the Numb locus was linked to Leber congenital amaurosis (LCA), a severe form of autosomal recessive retinal degeneration (Stockton et al., 1998). Although *SPATA7* was later identified as an LCA-causing gene in this region (Wang et al., 2009), it remains possible that unidentified mutations in *NUMB* contribute to LCA pathogenesis. Because Numb/NbL are essential for embryonic development, it is unlikely that null mutants exist in humans. Nonetheless, point mutations might affect Numb interaction with various cargos or endocytic proteins, altering normal Numb function in photoreceptors. Alternatively, mutations in *Cnga1*, which have been associated with retinitis pigmentosa in humans (Dryja et al., 1995), might modify its normal interaction with Numb, thereby disrupting localization of the channel that would lead to retinal degeneration, as we observed in the cDKO mouse. It will therefore be important to investigate whether the mutated forms of the Cng channel identified in human patients normally interact with Numb or not, as this could provide a molecular basis for the pathogenesis of the disease.

In primary cilia, a membrane diffusion barrier between the ciliary and plasma membrane prevents intermixing of proteins localized in the two domains (Nachury et al., 2010). A similar diffusion barrier was proposed to exist in photoreceptors, at the base of the connecting cilium, which link the IS to the OS (Nachury et al., 2010). Given that Numb promotes maintenance of diffusion barriers in epithelial cells (Sato et al., 2011), it appears plausible that barrier disruption could cause Cng channels to diffuse back into the IS in Numb/NbL cDKO photoreceptors. The overall levels of Cng channels in the OS, however, appear unchanged in the cDKO and after AAV-mediated gene inactivation, whereas they would be expected to decrease if the channel was free to diffuse back into the IS. Additionally, the IS plasma membrane protein Na<sup>+</sup>/K<sup>+</sup> ATPase does not diffuse into the OS of cDKO, as would be expected if a diffusion barrier was disrupted. Therefore, our data does not appear consistent with the possibility that Numb controls the integrity of diffusion barriers in photoreceptors.

Instead, our results favor a model in which Numb is acting as a key adaptor to regulate Cng channel trafficking and sorting. Our observation that Numb and the Cng channel subunits interact both *in vitro* and *in vivo* is consistent with this possibility. Because Numb localizes to the IS, and most of the Cng channels are found in the OS, it is likely that the interaction actually takes place transiently in the IS, along the trafficking route used by the Cng channel to the OS. Although we could not study the trafficking of Cng channels in photoreceptors due to technical difficulties, we provide evidence in a heterologous cell system that exogenous Numb overexpression promotes the delivery of Cnga1 to Rab11-positive recycling endosome. Interestingly, a recent study showed that rhodopsin also transits through the recycling endosome en route to the apical plasma membrane in polarized MDCK cells, and that Rab11 is required for the appropriate sorting of rhodopsin to the apical membrane (Thuenauer et al., 2014). Additionally, Rab11 is part of a “ciliary

targeting module” that regulate rhodopsin transport to the OS (Deretic and Wang, 2012). Rhodopsin trafficking, however, appears normal at P60 in the Numb/NbL cDKO photoreceptors, like other OS disk membrane proteins that we studied, excluding a direct role for Numb/NbL in disk membrane protein trafficking. Instead, our data suggest that Numb/NbL act as key regulators of OS plasma membrane protein sorting. Our observation that cone photoreceptors, which do not have an OS plasma membrane that is distinct from the disk membrane, do not stain for Numb is consistent with this possibility. In cDKO, the Cng channel is normally transported to the OS plasma membrane, but additionally accumulates on the IS plasma membrane. This observation indicates that Numb is required to prevent targeting of Cng channels to the IS, but not for its general delivery to the OS plasma membrane. We propose that Numb regulates the trafficking of Cng channels to the recycling endosome, where they can be properly sorted for specific delivery to the OS plasma membrane. In the absence of Numb, the Cng channels do not efficiently transit through the recycling endosome and cannot be sorted, such that they end up being delivered to the entire apical plasma membrane, comprising both the IS and OS (Fig. 7R). Whether Numb plays an active part in the sorting of Cng channels in the recycling endosome, or only promotes trafficking of the channel to the recycling endosome, will require future investigation.

In conclusion, we have identified a mechanism controlling the polarized delivery of Cng channels to the OS. Because OS disk membranes are normally trafficked in the absence of Numb, our results suggest that Numb may be specifically required for the sorting of proteins destined to the plasma membrane of OS. Considering that OS are specialized primary cilia, these results suggest that Numb might also be involved in regulating the trafficking proteins to other types of primary cilia.

## References

- Agarwal N, Nir I, Papermaster DS (1990) Opsin synthesis and mRNA levels in dystrophic retinas devoid of outer segments in retinal degeneration slow (rds) mice. *J Neurosci* 10:3275–3285. [Medline](#)
- Chinchore Y, Mitra A, Dolph PJ (2009) Accumulation of rhodopsin in late endosomes triggers photoreceptor cell degeneration. *PLoS Genet* 5:e1000377. [CrossRef Medline](#)
- Choudhury A, Dominguez M, Puri V, Sharma DK, Narita K, Wheatley CL, Marks DL, Pagano RE (2002) Rab proteins mediate Golgi transport of caveola-internalized glycosphingolipids and correct lipid trafficking in Niemann-Pick C cells. *J Clin Invest* 109:1541–1550. [CrossRef Medline](#)
- Connell G, Bascom R, Molday L, Reid D, McInnes RR, Molday RS (1991) Photoreceptor peripherin is the normal product of the gene responsible for retinal degeneration in the rds mouse. *Proc Natl Acad Sci U S A* 88:723–726. [CrossRef Medline](#)
- Cook NJ, Molday LL, Reid D, Kaupp UB, Molday RS (1989) The cGMP-gated channel of bovine rod photoreceptors is localized exclusively in the plasma-membrane. *J Biol Chem* 264:6996–6999. [Medline](#)
- Deretic D, Wang J (2012) Molecular assemblies that control rhodopsin transport to the cilia. *Vision Res* 75:5–10. [CrossRef Medline](#)
- Di Marcotullio L, Ferretti E, Greco A, De Smaele E, Po A, Sico MA, Alimandi M, Giannini G, Maroder M, Screpanti I, Gulino A (2006) Numb is a suppressor of hedgehog signalling and targets Gli1 for itch-dependent ubiquitination. *Nat Cell Biol* 8:1415–1423. [CrossRef Medline](#)
- Di Marcotullio L, Greco A, Mazzà D, Canettieri G, Pietrosanti L, Infante P, Coni S, Moretti M, De Smaele E, Ferretti E, Screpanti I, Gulino A (2011) Numb activates the E3 ligase itch to control Gli1 function through a novel degradation signal. *Oncogene* 30:65–76. [CrossRef Medline](#)
- Dryja TP, Finn JT, Peng YW, McGee TL, Berson EL, Yau KW (1995) Mutations in the gene encoding the alpha subunit of the rod cGMP-gated channel in autosomal recessive retinitis pigmentosa. *Proc Natl Acad Sci U S A* 92:10177–10181. [CrossRef Medline](#)
- Fariss RN, Molday RS, Fisher SK, Matsumoto B (1997) Evidence from normal and degenerating photoreceptors that two outer segment integral membrane proteins have separate transport pathways. *J Comp Neurol* 387:148–156. [CrossRef Medline](#)

- Flannery JG, Zolotukhin S, Vaquero MI, LaVail MM, Muzyczka N, Hauswirth WW (1997) Efficient photoreceptor-targeted gene expression *in vivo* by recombinant adeno-associated virus. *Proc Natl Acad Sci U S A* 94:6916–6921. [CrossRef Medline](#)
- Fox DA, Poblenz AT, He L (1999) Calcium overload triggers rod photoreceptor apoptotic cell death in chemical-induced and inherited retinal degenerations. *Ann N Y Acad Sci* 893:282–285. [CrossRef Medline](#)
- Hartong DT, Berson EL, Dryja TP (2006) Retinitis pigmentosa. *Lancet* 368:1795–1809. [CrossRef Medline](#)
- Hicks D, Molday RS (1986) Differential immunogold dextran labeling of bovine and frog rod and cone cells using monoclonal-antibodies against bovine rhodopsin. *Exp Eye Res* 42:55–71. [CrossRef Medline](#)
- Hüttel S, Michalakakis S, Seeliger M, Luo DG, Acar N, Geiger H, Hudl K, Mader R, Haverkamp S, Moser M, Pfeifer A, Gerstner A, Yau KW, Biel M (2005) Impaired channel targeting and retinal degeneration in mice lacking the cyclic nucleotide-gated channel subunit CNGB1. *J Neurosci* 25:130–138. [CrossRef Medline](#)
- Illing M, Molday LL, Molday RS (1997) The 220-kDa Rim protein of retinal rod outer segments is a member of the ABC transporter superfamily. *J Biol Chem* 272:10303–10310. [CrossRef Medline](#)
- Insinna C, Besharse JC (2008) Intraflagellar transport and the sensory outer segment of vertebrate photoreceptors. *Dev Dyn* 237:1982–1992. [CrossRef Medline](#)
- Juven-Gershon T, Shifman O, Unger T, Elkeles A, Haupt Y, Oren M (1998) The Mdm2 oncoprotein interacts with the cell fate regulator Numb. *Mol Cell Biol* 18:3974–3982. [Medline](#)
- Kechad A, Jolicoeur C, Tufford A, Mattar P, Chow RW, Harris WA, Cayouette M (2012) Numb is required for the production of terminal asymmetric cell divisions in the developing mouse retina. *J Neurosci* 32:17197–17210. [CrossRef Medline](#)
- Kizhatil K, Baker SA, Arshavsky VY, Bennett V (2009) Ankyrin-G promotes cyclic nucleotide-gated channel transport to rod photoreceptor sensory cilia. *Science* 323:1614–1617. [CrossRef Medline](#)
- Le YZ, Zheng L, Zheng W, Ash JD, Agbaga MP, Zhu M, Anderson RE (2006) Mouse opsin promoter-directed Cre recombinase expression in transgenic mice. *Mol Vis* 12:389–398. [Medline](#)
- Lee ES, Burnside B, Flannery JG (2006) Characterization of peripherin/rdns and rom-1 transport in rod photoreceptors of transgenic and knockout animals. *Invest Ophthalmol Vis Sci* 47:2150–2160. [CrossRef Medline](#)
- Li T (2001) Disease model: photoreceptor degenerations. *Trends Mol Med* 7:133–135. [CrossRef Medline](#)
- Matsuda T, Cepko CL (2004) Electroporation and RNA interference in the rodent retina *in vivo* and *in vitro*. *Proc Natl Acad Sci U S A* 101:16–22. [CrossRef Medline](#)
- McGill MA, McGlade CJ (2003) Mammalian numb proteins promote Notch1 receptor ubiquitination and degradation of the Notch1 intracellular domain. *J Biol Chem* 278:23196–23203. [CrossRef Medline](#)
- McGill MA, Dho SE, Weinmaster G, McGlade CJ (2009) Numb regulates post-endocytic trafficking and degradation of Notch1. *J Biol Chem* 284:26427–26438. [CrossRef Medline](#)
- Mears AJ, Kondo M, Swain PK, Takada Y, Bush RA, Saunders TL, Sieving PA, Swaroop A (2001) Nr1 is required for rod photoreceptor development. *Nat Genet* 29:447–452. [CrossRef Medline](#)
- Moritz OL, Molday RS (1996) Molecular cloning, membrane topology, and localization of bovine rom-1 in rod and cone photoreceptor cells. *Invest Ophthalmol Vis Sci* 37:352–362. [Medline](#)
- Nachury MV, Seeley ES, Jin H (2010) Trafficking to the ciliary membrane: how to get across the periciliary diffusion barrier? *Annu Rev Cell Dev Biol* 26:59–87. [CrossRef Medline](#)
- Nie J, McGill MA, Dermer M, Dho SE, Wolting CD, McGlade CJ (2002) LNX functions as a RING type E3 ubiquitin ligase that targets the cell fate determinant Numb for ubiquitin-dependent degradation. *EMBO J* 21:93–102. [CrossRef Medline](#)
- Nir I, Papermaster DS (1989) Immunocytochemical localization of opsin in degenerating photoreceptors of RCS rats and rd and rds mice. *Prog Clin Biol Res* 314:251–264. [Medline](#)
- Nir I, Agarwal N, Papermaster DS (1990) Opsin gene expression during early and late phases of retinal degeneration in rds mice. *Exp Eye Res* 51:257–267. [CrossRef Medline](#)
- Papermaster DS (2002) The birth and death of photoreceptors: the Friedenwald lecture. *Invest Ophthalmol Vis Sci* 43:1300–1309. [Medline](#)
- Petersen PH, Zou K, Hwang JK, Jan YN, Zhong W (2002) Progenitor cell maintenance requires numb and numbl like during mouse neurogenesis. *Nature* 419:929–934. [CrossRef Medline](#)
- Petersen PH, Zou K, Krauss S, Zhong W (2004) Continuing role for mouse Numb and Numbl in maintaining progenitor cells during cortical neurogenesis. *Nat Neurosci* 7:803–811. [CrossRef Medline](#)
- Qiu L, Joazeiro C, Fang N, Wang HY, Elly C, Altman Y, Fang D, Hunter T, Liu YC (2000) Recognition and ubiquitination of Notch by itch, a hec-type E3 ubiquitin ligase. *J Biol Chem* 275:35734–35737. [CrossRef Medline](#)
- Ramarurthy V, Cayouette M (2009) Development and disease of the photoreceptor cilium. *Clin Genet* 76:137–145. [CrossRef Medline](#)
- Rasin MR, Gazula VR, Breunig JJ, Kwan KY, Johnson MB, Liu-Chen S, Li HS, Jan LY, Jan YN, Rakic P, Sestan N (2007) Numb and Numbl are required for maintenance of cadherin-based adhesion and polarity of neural progenitors. *Nat Neurosci* 10:819–827. [CrossRef Medline](#)
- Rattner A, Smallwood PM, Williams J, Cooke C, Savchenko A, Lyubarsky A, Pugh EN, Nathans J (2001) A photoreceptor-specific cadherin is essential for the structural integrity of the outer segment and for photoreceptor survival. *Neuron* 32:775–786. [CrossRef Medline](#)
- Rodriguez-Boulau E, Macara IG (2014) Organization and execution of the epithelial polarity programme. *Nat Rev Mol Cell Biol* 15:225–242. [CrossRef Medline](#)
- Salcini AE, Confalonieri S, Doria M, Santolini E, Tassi E, Minenkova O, Cesareni G, Pelicci PG, Di Fiore PP (1997) Binding specificity and *in vivo* targets of the EH domain, a novel protein-protein interaction module. *Genes Dev* 11:2239–2249. [CrossRef Medline](#)
- Santolini E, Puri C, Salcini AE, Gagliani MC, Pelicci PG, Tacchetti C, Di Fiore PP (2000) Numb is an endocytic protein. *J Cell Biol* 151:1345–1352. [CrossRef Medline](#)
- Sato K, Watanabe T, Wang S, Kakeno M, Matsuzawa K, Matsui T, Yokoi K, Murase K, Sugiyama I, Ozawa M, Kaibuchi K (2011) Numb controls E-cadherin endocytosis through p120 catenin with aPKC. *Mol Biol Cell* 22:3103–3119. [CrossRef Medline](#)
- Stockton DW, Lewis RA, Abboud EB, Al-Rajhi A, Jabak M, Anderson KL, Lupski JR (1998) A novel locus for Leber congenital amaurosis on chromosome 14q24. *Hum Genet* 103:328–333. [CrossRef Medline](#)
- Sung CH, Chuang JZ (2010) The cell biology of vision. *J Cell Biol* 190:953–963. [CrossRef Medline](#)
- Susini L, Passer BJ, Amzallag-Elbaz N, Juven-Gershon T, Prieur S, Privat N, Tuynder M, Gendron MC, Israël A, Amson R, Oren M, Telerman A (2001) Siah-1 binds and regulates the function of Numb. *Proc Natl Acad Sci U S A* 98:15067–15072. [CrossRef Medline](#)
- Thuenauer R, Hsu YC, Carvajal-Gonzalez JM, Deborde S, Chuang JZ, Römer W, Sonnleitner A, Rodriguez-Boulau E, Sung CH (2014) Four-dimensional live imaging of apical biosynthetic trafficking reveals a post-Golgi sorting role of apical endosomal intermediates. *Proc Natl Acad Sci U S A* 111:4127–4132. [CrossRef Medline](#)
- Vallazza-Deschamps G, Cia D, Gong J, Jellali A, Duboc A, Forster V, Sahel JA, Tessier LH, Picaud S (2005) Excessive activation of cyclic nucleotide-gated channels contributes to neuronal degeneration of photoreceptors. *Eur J Neurosci* 22:1013–1022. [CrossRef Medline](#)
- Wang H, den Hollander AI, Moayed Y, Abulimiti A, Li Y, Collin RW, Hoyng CB, Lopez I, Abboud EB, Al-Rajhi AA, Bray M, Lewis RA, Lupski JR, Mardon G, Koeneke RK, Chen R (2009) Mutations in SPATA7 cause Leber congenital amaurosis and juvenile retinitis pigmentosa. *Am J Hum Genet* 84:380–387. [CrossRef Medline](#)
- Wilson A, Ardiet DL, Saner C, Vilain N, Beermann F, Aguet M, Macdonald HR, Zilian O (2007) Normal hemopoiesis and lymphopoiesis in the combined absence of numb and numbl like. *J Immunol* 178:6746–6751. [CrossRef Medline](#)
- Zhang Y, Molday LL, Molday RS, Sarfare SS, Woodruff ML, Fain GL, Kraft TW, Pittler SJ (2009) Knockout of GARP and the beta-subunit of the rod cGMP-gated channel disrupts disk morphogenesis and rod outer segment structural integrity. *J Cell Sci* 122:1192–1200. [CrossRef Medline](#)
- Zhong H, Molday LL, Molday RS, Yau KW (2002) The heteromeric cyclic nucleotide-gated channel adopts a 3A:1B stoichiometry. *Nature* 420:193–198. [CrossRef Medline](#)
- Zhong W, Jiang MM, Schonemann MD, Meneses JJ, Pedersen RA, Jan LY, Jan YN (2000) Mouse numb is an essential gene involved in cortical neurogenesis. *Proc Natl Acad Sci U S A* 97:6844–6849. [CrossRef Medline](#)
- Zilian O, Saner C, Hagedorn L, Lee HY, Säuberli E, Suter U, Sommer L, Aguet M (2001) Multiple roles of mouse Numb in tuning developmental cell fates. *Curr Biol* 11:494–501. [CrossRef Medline](#)